Active Multiband Printed Antennas for Mobile Communications

Ridwan Sulemangi Gulamo Nabi

***Abstract* – The goal of this paper is to study small size multiband reconfigurable antennas and to develop miniaturization techniques. The paper presents results for return loss and radiation pattern of novel small sized patch antennas adequate for frequency reconfigurability.**

***Index terms* – Reconfigurable antennas; multifrequency antennas; triple band antennas; microstrip antennas; miniaturization; parasitic element.**

I. Introduction

Reconfigurable antennas have been the subject of many studies on the recent years. These antennas have the capacity of changing their behavior when the switches are on or off. They can have reconfigurable polarization, frequency of operation or radiation pattern.

Antennas with reconfigurable polarization [1] – [4] can be used to improve channel capacity and reduce the crosstalk level on communications.

Antennas with reconfigurable frequency [5] – [8] are the most studied because they allow the same antenna to work in different services in different parts of the frequency spectrum.

Antennas with reconfigurable radiation pattern [9] – [12] can be used to avoid noise sources or intentional jamming, improve security by directing the signal only to intended users, and expand the capacity of beam control on large phased arrays.

Initially in the present work, a square antenna with two parasitic elements was studied, for operation in three frequency bands. Then, a triangular antenna obtained by cutting the square antenna by its diagonal line that contains the feeding, was studied. This cut was made to try to obtain a PIFA [13] (Planar Inverted F Antenna), but it was seen in the simulation that the antenna worked better without the shorting pins, so this resulted in a new kind of miniaturization technique.

First, the triple band triangular antenna was designed with ideal switches which were modeled as metal strips; a prototype was fabricated and measured. In a second step, the antenna dimensions were readjusted for operation with real switches that on this case are PIN diodes. This part of the study was based only on simulations.

II. Test configurations

The first antennas were designed to test a new approach for miniaturization, on the lower TDD band of UMTS. The tests were made on antennas with simple shapes: a square antenna with central feeding (Fig. 1), a square antenna with diagonal feeding (Fig. 5), a triangle antenna (Fig. 6) and a circle antenna (Fig. 7). The antennas were modified by cutting through the symmetry axis, and readjusting the dimensions to correct the band shift that happened because of the cut. The size reductions are of 47.9 %, 49.5 %, 45.8 % and 51.3 % on the size compared with the original square antenna with central feeding, square antenna with diagonal feeding, triangle antenna and circle antenna, respectively.

On the figures showing the geometry of the antennas, the outer shape represents the ground plane.

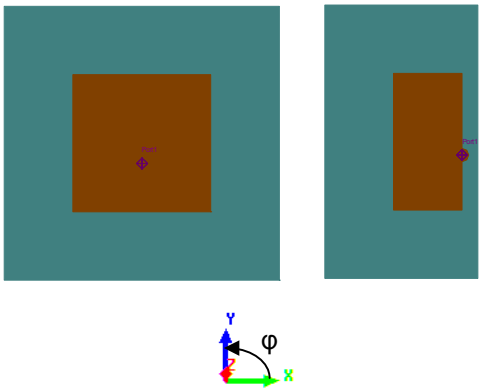

Fig. 1. Geometry of the square antenna with central feeding and the cut version. The side of the square antenna is 51.5 mm, and the bigger side of the cut antenna is 52.55 mm.

Fig. 2 shows the results for the square antenna with central feeding the cut version. We can see that the resonance frequency is practically coincident although with a slight reduction in the bandwidth which is acceptable in view of the reduction on the size.

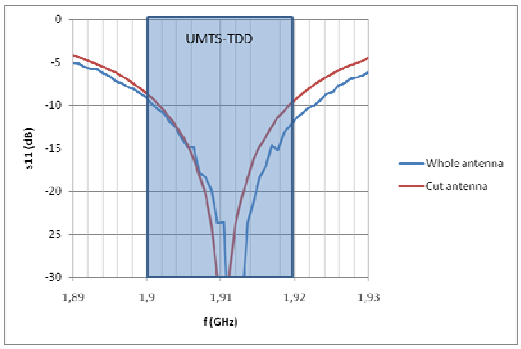

Fig. 2. Return losses for the square antenna with central feeding and the cut version.

Fig. 3 and Fig. 4 show the radiation patterns of the square antenna with central feeding and the cut versions. The reduction of the difference between the co-polar and cross-polar happens because the symmetry is lost when the cut is made. On the whole antenna there was a cancelation of the symmetric components of the field, and that is lost when the antenna is cut.

On these diagrams the E and H planes intercepts the plane of the antenna with an angle $\varphi = 90^{o}$ and $\varphi = 0^{o}$ respectively.

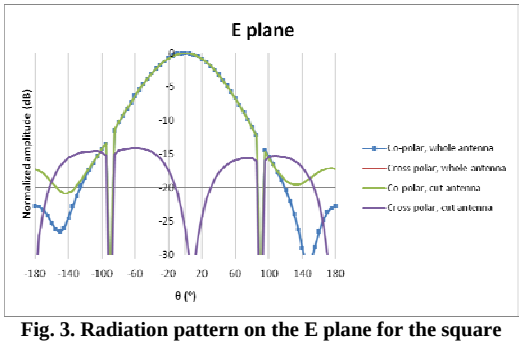

Fig. 3. Radiation pattern on the E plane for the square antenna with central feeding and the cut version.

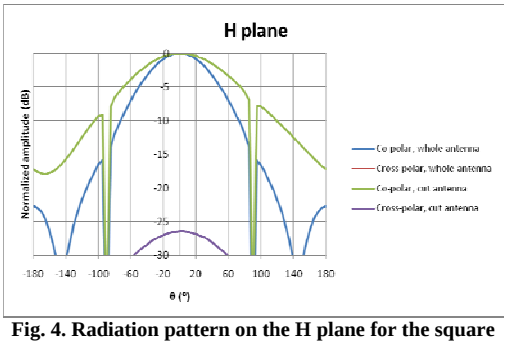

Fig. 4. Radiation pattern on the H plane for the square antenna with central feeding and the cut version.

Fig. 5 to Fig. 7 show the other test configurations used. The results are omitted because the conclusions are similar that the ones made for the square antenna with central feeding.

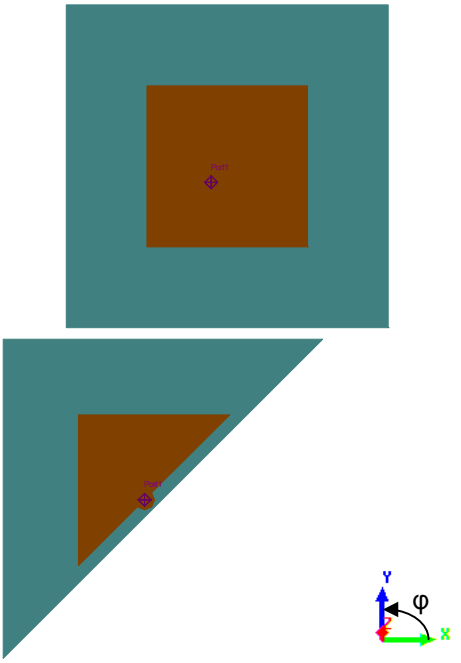

Fig. 5. Geometry of the square antenna with diagonal feeding and the cut version. The side of the square antenna is 51.5 mm, and the bigger side of the cut antenna is 51.779 mm

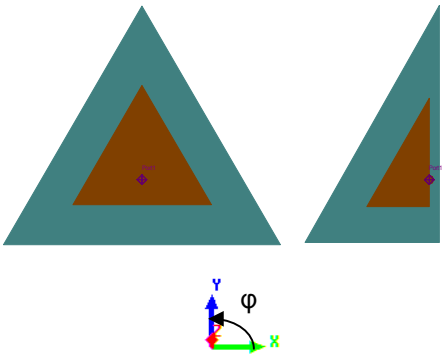

Fig. 6. Geometry of the triangular antenna and the cut version. The side of the triangular antenna on the left is 68.8 mm, and the bigger side of theantenna on the right is 71.6 mm.

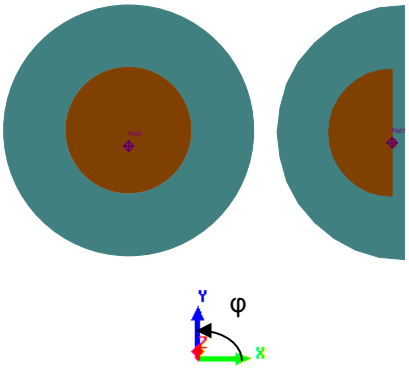

Fig. 7. Geometry of the circular antenna and the cut version. The radius of the circular antenna is 31.75 mm. and the radius of the semi-circular antenna is 31.34 mm.

III. Antennas with ideal switches

After cutting by its diagonal line, that contains the feeding, a square antenna with ideal switches with two parasitic elements (Fig. 8 and Fig. 9), it is obtained a triangular antenna with ideal switches (Fig. 10 - Fig. 15). with a reduction in 51.8 % of the area, compared with the square one. The cut is made by the diagonal line because the feeding is on this line, therefore, is the symmetry axis of the antenna. To test the reconfigurable triangular antennas with ideal switches, three prototypes were designed: the first, with all switches ON was for the lower TDD band of UMTS; the second, with only the inner switches ON was for Bluetooth, and the third, with all switches OFF was for the WiMAX test frequencies in Portugal.

The square antenna with diagonal feeding was chosen because, out of the studied geometries, it is the most balanced option in terms of area and bandwidth. A triple band antenna is obtained by taking this geometry, framing it by two parasitic elements, and connecting all of them by switches.

On the triple band triangular antenna, besides the cut, other alterations were introduced: it was necessary a semi-circle, of radius 2.5 mm to surround the feeding point. In order to cover the area of this semi-circle, the near edge of the ground plane was extended by 6 mm. With the cut, the feeding point is very close to the edge of the antenna, so it was necessary to use a microstrip transmission line to connect the coaxial cable to the feeding position. This avoids positioning the coaxial cable near the edge of he antenna thus reducing the influence of its physical presence.

To tune the antennas, two parameters were used for each active patch (on this paper “active patch” refers to the part of the antenna connected to the feeding at each configuration): the size of the active patch was used to shift the band into lower or higher frequencies, and the relative position of feeding of each active patch was used to change the impedance and therefore to get a better resonance.

In some figures, to see the details more clearly, the ground plane and the microstrip transmission line were omitted. The side length on the ground plane is the double of the side length of the antennas patch. The slots are 0.5 mm wide and the ideal switches are 1 mm wide.

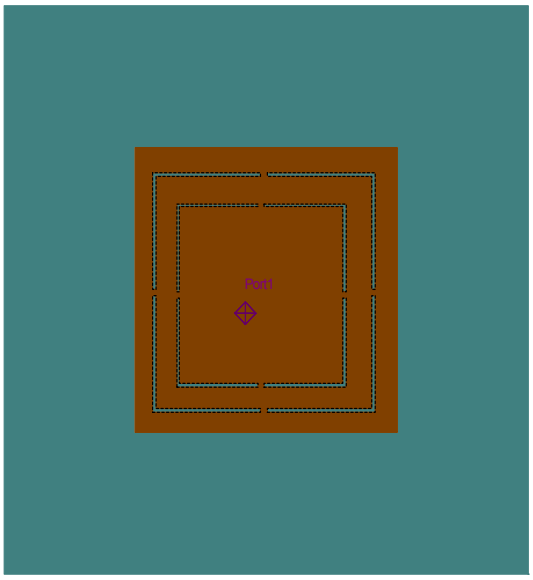

Fig. 8. Geometry of the configuration 1 of the square antenna with ideal switches. The side of the antenna is 43.7 mm.

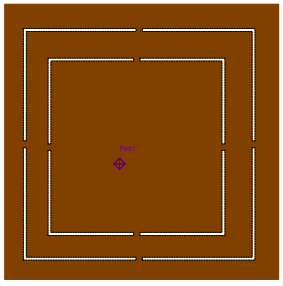

(C1)

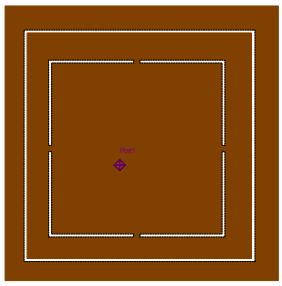

(C2)

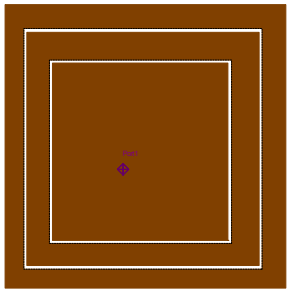

(C3)

Fig. 9. Details of the three configurations (C1, C2,C3) of the square antenna with ideal switches.

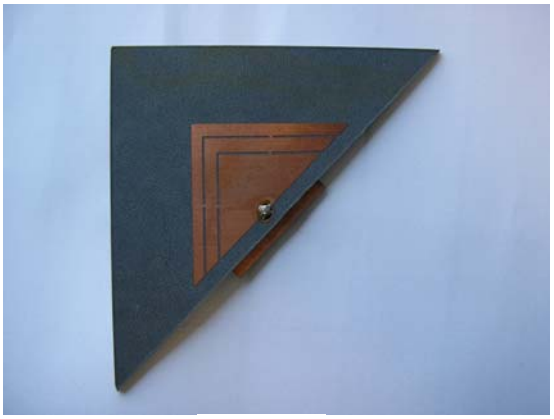

Fig. 10. Photograph of the prototype of the configuration 1 of the triangular antenna with ideal switches. The smaller sides of the antenna are 42.9 mm.

Fig. 11. Photograph of the back side of the prototype of the triangular antenna with ideal switches. In this image we can see the coaxial cable and the microstrip transmission line.

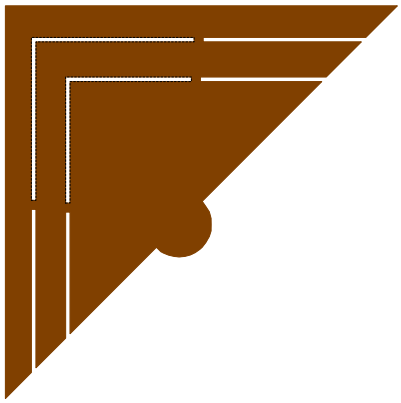

Fig. 12. Detail of the configuration 1 of the triangular antenna with ideal switches.

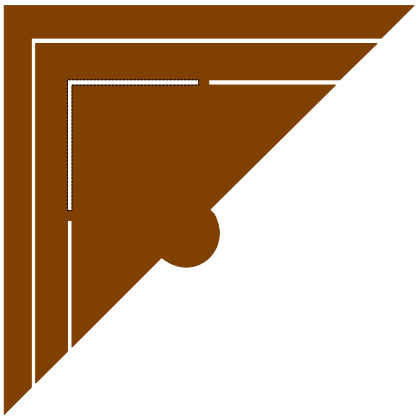

Fig. 13. Details of the configuration 2 of the triangular antenna with ideal switches.

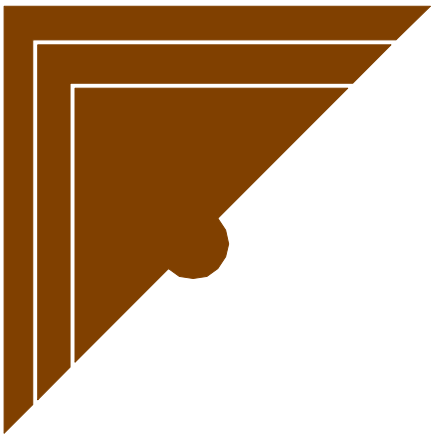

Fig. 14. Details of the configuration 3 of the triangular antenna with ideal switches.

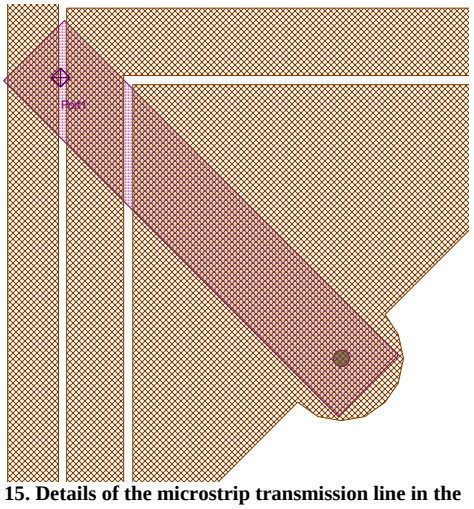

Fig. 15. Details of the microstrip transmission line in the configuration 3 of the triangular antenna with ideal switches.

Fig. 16, Fig. 17 and Fig. 18 show the comparison between the simulation and measurement of the triangular antenna with ideal switches. The largest shift was on the WiMAX frequency, but on the rest the results show reasonable agreement with the simulations.

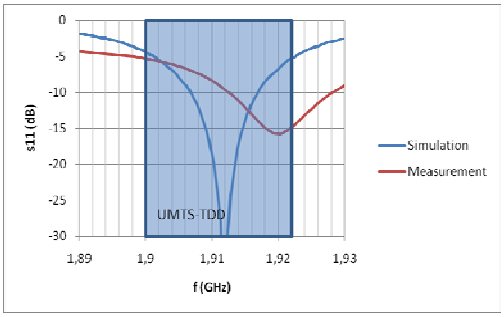

Fig. 16. Comparison between simulations and experimental results for the UMTS band, for the triangular antenna with ideal switches.

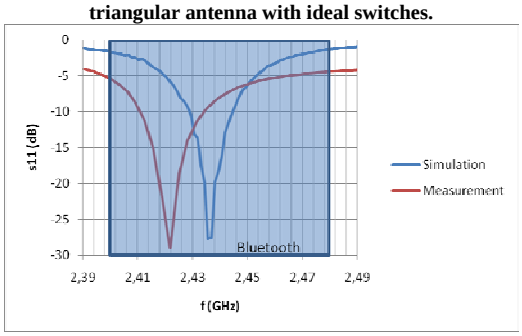

Fig. 17. Comparison between simulations and experimental results for the Bluetooth band, for the triangular antenna with ideal switches.

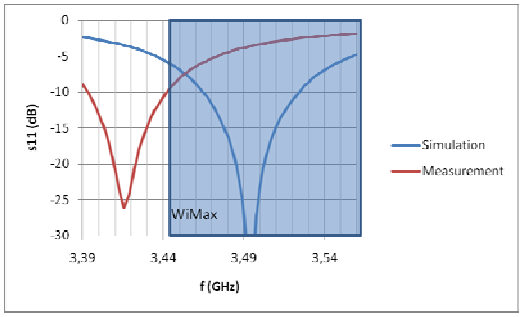

Fig. 18. Comparison between simulations and experimental results for the WiMAX band, for the triangular antenna with ideal switches.

Fig. 19 to Fig. 24 show the radiation patterns for the triangular antenna with ideal switches. The difference between simulation and measurement might be because of the coaxial cable interference, which is not taken in consideration by the simulation program. On these figures, the E and H planes intercepts the plane of the antenna with an angle $\varphi = 45^{o}$ and $\varphi = 135^{o}$ respectively.

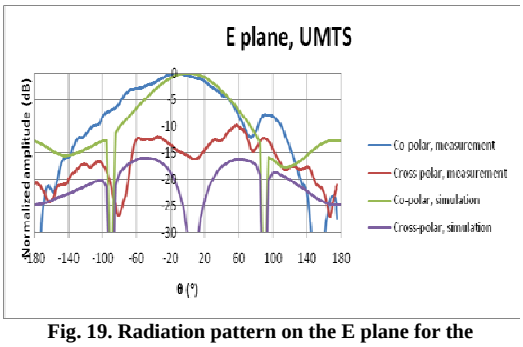

Fig. 19. Radiation pattern on the E plane for the triangular antenna with ideal switches, on the UMTS band.

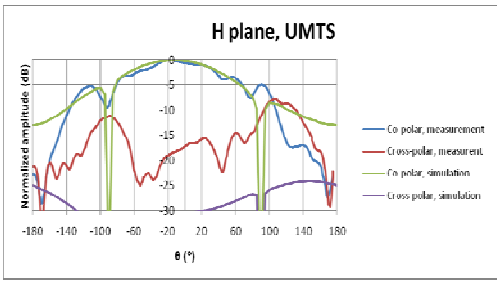

Fig. 20. Radiation pattern on the H plane for the triangular antenna with ideal switches, on the UMTS band.

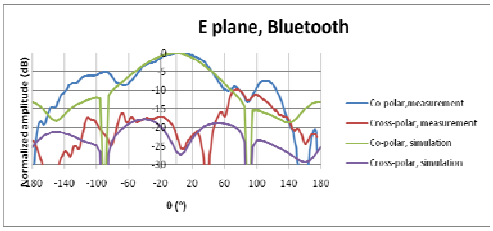

Fig. 21. Radiation pattern on the E plane for the triangular antenna with ideal switches, on the Bluetooth band.

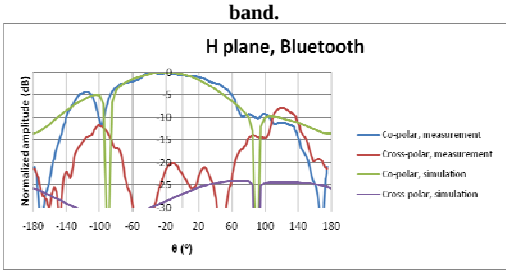

Fig. 22. Radiation pattern on the H plane for the triangular antenna with ideal switches, on the Bluetooth band.

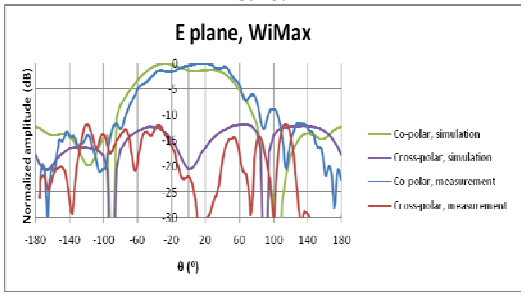

Fig. 23. Radiation pattern on the E plane for the triangular antenna with ideal switches, on the WiMAX band.

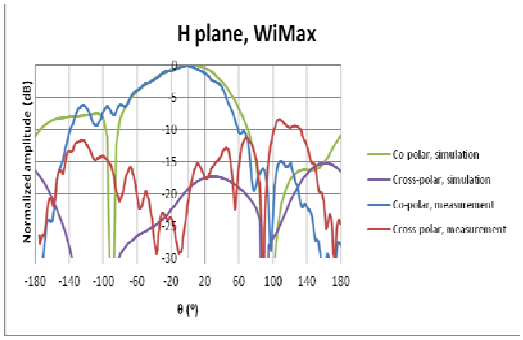

Fig. 24. Radiation pattern on the H plane for the triangular antenna with ideal switches, on the WiMAX band.

IV. Antenna with real switches

To simulate the antenna with real switches (Fig. 25), it was necessary to extract experimentally the *s* parameters of the PIN diode. The BAR50-02V from *Infineon* was selected. Fig. 26 shows the details of the positions of the diodes on the antenna.

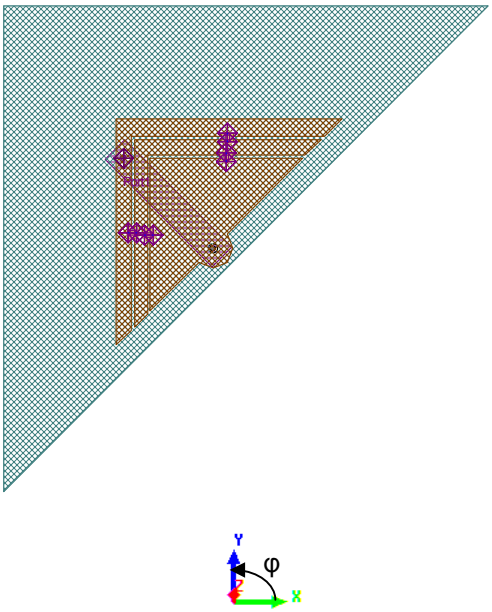

Fig. 25. Geometry of the triangular antenna with real switches. The smaller sides of the antenna are 42 mm.

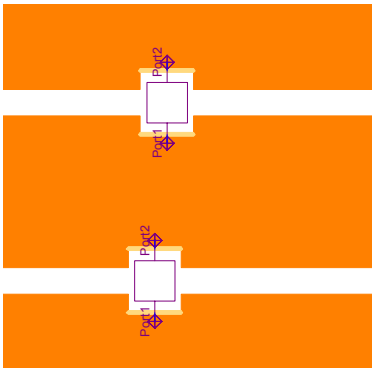

Fig. 26. Detail of the switches used for the simulations.

Fig. 27, Fig. 28 and Fig. 29 show the comparison between the simulations of the triangular antenna with real and ideal switches. There is a significant difference because of the parasitic capacity of the PIN diodes.

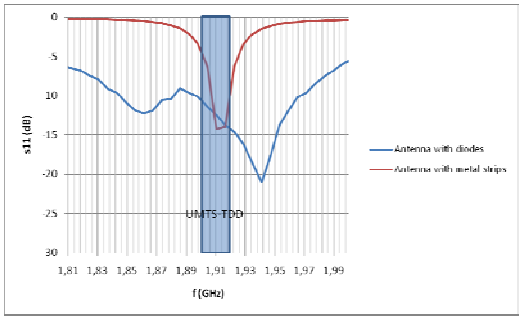

Fig. 27. Comparison between the simulations of the triangular antennas with ideal and real switches for the UMTS band.

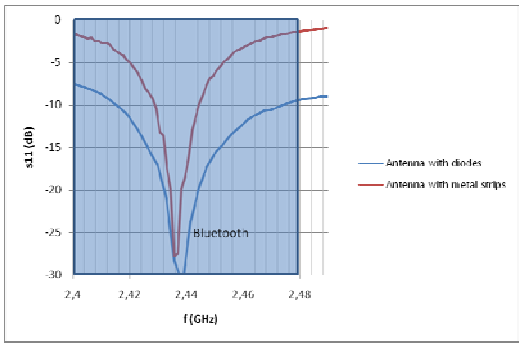

Fig. 28. Comparison between the simulations of the triangular antennas with ideal and real switches for the Bluetooth band.

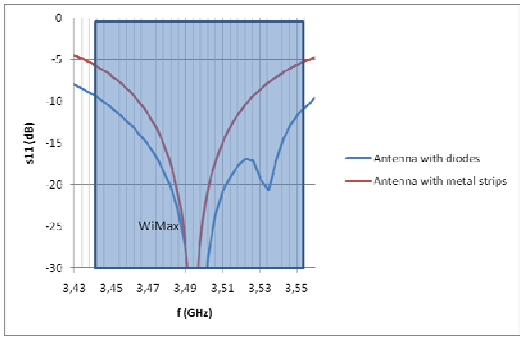

Fig. 29. Comparison between the simulations of the triangular antennas with ideal and real switches for the WiMAX band.

Fig. 30 and Fig. 31 show the simulated radiation patterns of the triangular antenna with real switches. On the UMTS band, the E and H planes intercepts the plane of the antenna with an angle φ = 25º and φ = 115º respectively, on the Bluetooth band the E and H planes intercepts the plane of the antenna with an angle φ = 35º and φ = 125º respectively and on the WiMAX band the E and H planes intercepts the plane of the antenna with an angle φ = 30º and φ = 120º respectively.

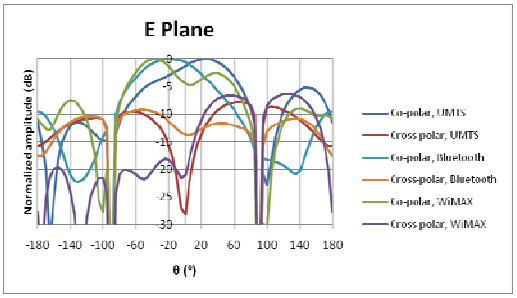

Fig. 30. Radiation pattern on the E plane for the triangular antenna with real switches.

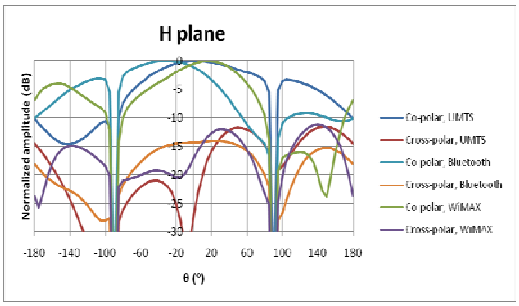

Fig. 31. Radiation pattern on the H plane for the triangular antenna with real switches.

V. Conclusion

On this paper it was studied the viability of using a triple band reconfigurable antenna with a strategy of size reduction.

Tests were made to verify if the new concept of area reduction is valid. The results were satisfactory, obtaining great area reductions but with some penalizations on the isolation between the two orthogonal components of the polarization.

The objective of obtaining a triple band antenna with small size was obtained, but it was not possible to build a prototype with real switches. The future work consists on replacing the PIN diodes for switches with better insulation and lower insertion losses, the RF-MEMS, and to obtain a larger bandwidth on the Bluetooth band.

References

[1] Nanbo, Jin, Yang, F., Rahmat-Samii, Y.
"A Novel Reconfigurable Patch Antenna with both frequency and polarization diversities for wireless communication".
Antennas and Propagation Society International Symposium, 2004,IEEE, Vol. 2, 20-25 June 2004, pp.1796 – 1799.

[2] Jin, N.; Fan Yang; Rahmat-Samii, Y.
"A novel patch antenna with switchable slot (PASS): dual-frequency operation with reversed circular polarizations".
Antennas and Propagation, IEEE Transactions on Volume 54, Issue 3, March 2006 Page(s):1031 – 1034.

[3] Shynu, S. V., Augustin, G., Aanandan, C. K., Mohanan, P., Vasudevan , K.
"Development of a varactor-controlled dual-frequency reconfigurable microstrip antenna".
Microwave and Optical Technology Letters, Vol.46, No. 4, 20 August 2005, pp.375-377.

[4] Simons, R.N.; Donghoon Chun; Katehi, L.P.B.
"Polarization reconfigurable patch antenna using microelectromechanical systems (MEMS) actuators".
Antennas and Propagation Society International Symposium, 2002. IEEE
Volume 2, 16-21 June 2002 Page(s):6 - 9 vol.2.

[5] Onat, S., Alatan, L., Demir, S., Unlu, M., Akin, T.
"Design of a Re-Configurable Dual Frequency Microstrip Antenna with Integrated RF MEMS Switches".
Antennas and Propagation Society International Symposium, 2005. IEEE, Vol. 2A, 3-8 July, pp. 384 – 387.

[6] Lee, A.W.M., Kagan, S.K., Wong, M., Singh, R.S., Brown, E.R.
"Measurement and FEM modeling of a reconfigurable-patch antenna for use in the wideband gapfiller satellite system".
Antennas and Propagation Society International Symposium, 2003. IEEE, Vol. 1, 22-27 June 2003, pp. 379 – 382.

[7] Liu, S., Lee, M., Jung, C., Li, G.P., Flaviis, F.

"A Frequency-Reconfigurable Circularly Polarized Patch Antenna by Integrating MEMS Switches".
Antennas and Propagation Society International Symposium, 2005. IEEE, Vol. 2A, 3-8 July, pp. 413 – 416.

[8] Simons, R.N.; Donghoon Chun; Katehi, L.P.B.
"Reconfigurable array antenna using microelectromechanical systems (MEMS) actuators".
Antennas and Propagation Society International Symposium, 2001. IEEE
Volume 3, 8-13 July 2001 Page(s):674 - 677 vol.3.

[9] Chang, B.C.C.; Qian, Y.; Itoh, T.
"A reconfigurable leaky mode/patch antenna controlled by PIN diode switches".
Antennas and Propagation Society International Symposium, 1999. IEEE
Volume 4, 11-16 July 1999 Page(s):2694 - 2697 vol.4.

[10] Qian, Y.; Chang, B.C.C.; Chang, M.F.; Itoh, T.
"Reconfigurable leaky-mode/multifunction patch antenna structure".
Electronics Letters
Volume 35, Issue 2, 21 Jan. 1999 Page(s):104 – 105.

[11] Kunda, V.K.; Ali, M.
"Reconfigurable stacked patch antenna for satellite and terrestrial applications".
Wireless Communication Technology, 2003. IEEE Topical Conference on.
15-17 Oct. 2003 Page(s):152 – 153.

[12] Xue-Song Yang; Bing-Zhong Wang; Weixia Wu.
"Pattern reconfigurable patch antenna with two orthogonal quasi-Yagi arrays".
Antennas and Propagation Society International Symposium, 2005 IEEE.
Volume 2B, 3-8 July 2005 Page(s):617 - 620 vol. 2B.

[13] Jung, M., Kim, Y., and Lee, B.
"Dual frequency meandered PIFA for Bluetooth and WLAN applications".
IEEE AP-S Int. Symp., Columbus, OH, USA, 2003.